Materials Research Express

INCLUSIVE PUBLISHING TRUSTED SCIENCE
PURPOSE-LED PUBLISHING™

PAPER • **OPEN ACCESS**

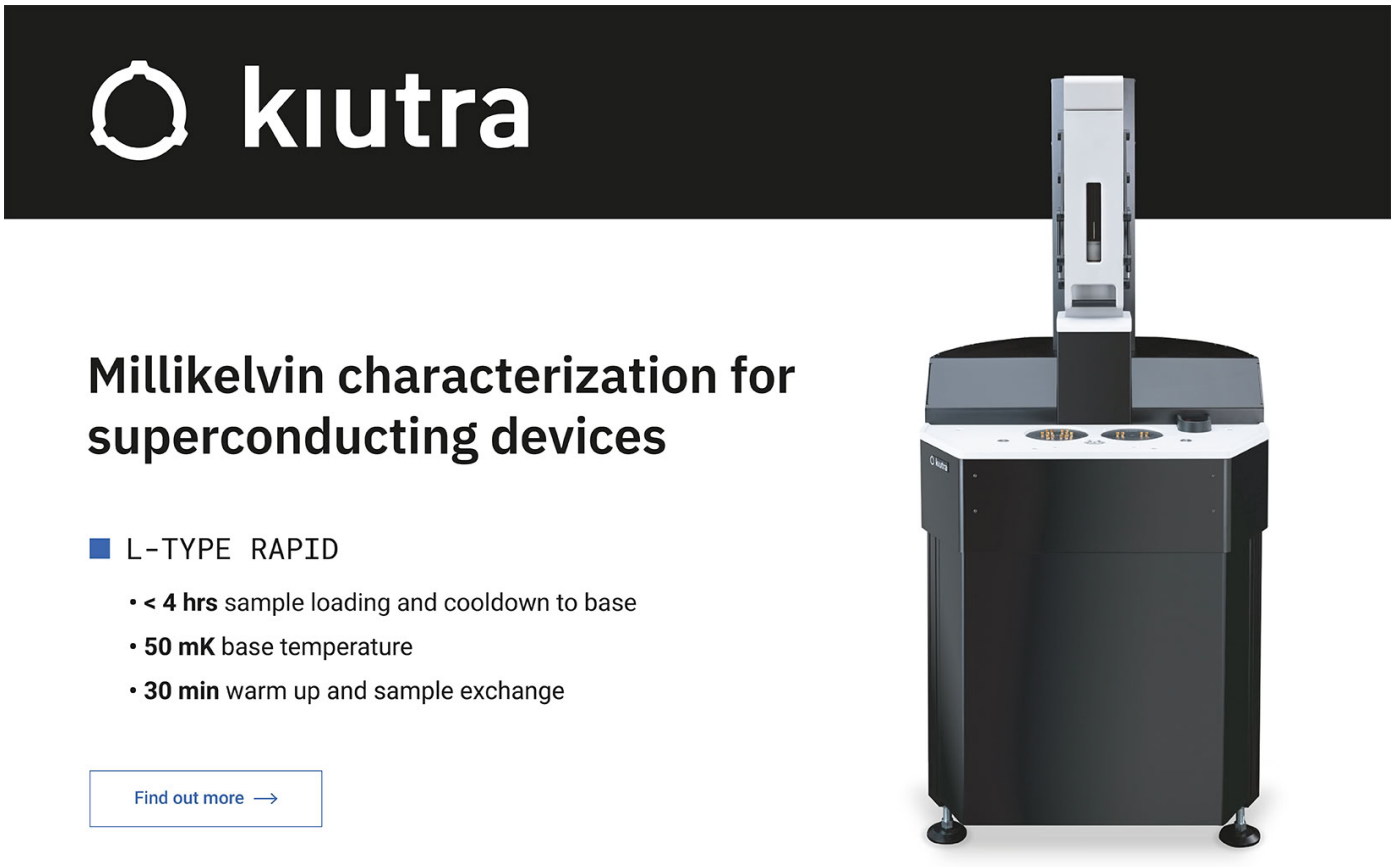
The effect of zircon particle size on the surface properties of sanitaryware glaze

To cite this article: Gülsüm Topateş *et al* 2020 *Mater. Res. Express* **7** 015203

View the article online for updates and enhancements.

You may also like

- Ultra-dense (Bi, V, B)-oxide-added zircon ceramics fabricated by liquid-phase assisted spark plasma sintering (SPS)
Musyarofah Musyarofah, Yuliani P Sari, Allif R Hilmi et al.
- Modelling of optically stimulated luminescence of zircon: assessment of the suitability for dating
A A Turkin, D I Vainshtein and H W den Hartog
- Effect of substitutional impurities on vibrational properties of zircon: a first-principles study
Natalya Sheremetyeva, Daniele J Cherniak, E Bruce Watson et al.



This content was downloaded from IP address 79.123.165.30 on 01/10/2026 at 14:09

Materials Research Express

PAPER

The effect of zircon particle size on the surface properties of sanitaryware glaze

Gülsüm Topateş[1], **Burak Alıcı**[1], **Baran Tarhan**[2] **and Müge Tarhan**[2]

[1] Ankara Yıldırım Beyazıt University, Faculty of Engineering and Natural Sciences, Department of Metallurgical and Materials Engineering, 06010, Keçiören, Ankara, Turkey
[2] Uşak University, Faculty of Fine Arts, Ceramic Department, 64000, Uşak, Turkey

E-mail: gtopates@ybu.edu.tr

Keywords: submicron zircon, sanitaryware glaze, surface properties, bacterial activity

OPEN ACCESS

RECEIVED
14 October 2019

REVISED
5 December 2019

ACCEPTED FOR PUBLICATION
24 December 2019

PUBLISHED
13 January 2020

Original content from this work may be used under the terms of the Creative Commons Attribution 4.0 licence.

Any further distribution of this work must maintain attribution to the author(s) and the title of the work, journal citation and DOI.

Abstract

Zircon (zirconium silicate; $ZrSiO_4$) is an essential compound of sanitaryware glaze due to contributions to the final properties of the surface. In this study, the effect of zircon particle size on the surface properties (microstructural development, opacity, roughness, hardness and bacterial activity) were studied. Initially, zircon powder was milled by planetary mill at different times (0–25 min) and added to an industrial sanitaryware glaze recipe. Four different glaze suspensions were prepared, applied to a sanitary ware body and sintered in an industrial tunnel kiln at 1220 °C for 16 h. The effect of milling is clearly observed via SEM investigations by uniform distribution of zircon grains with a size reduction to 0.38 μm. This uniform distribution and reduction in particle size provides improvements in opacity (L^* value measured as 91.47) and hardness (Hv was 6.3 ($\pm$0.3) GPa) values. According to AFM studies, the average roughness decreased to 10.94 nm when a 25 min milling process was used. The antibacterial activities of two samples (milled for 0 and 25 min) were analyzed against Escherichia coli and Staphylococcus aureus. Although both samples did not show any antibacterial activity, the number of viable bacteria on the samples milled for 25 min decreased drastically compared to the one not milled. A smoother glaze surface facilitated less sites for adherence and accommodation of bacteria and hence a decrease in bacterial colonization was obtained.

1. Introduction

Several functions of sanitaryware, such as corrosion-wear resistance, dirt repellency, cleanability, optical properties and antibacterial activity are directly related to the surface characteristics of glazes. Since expectations on the quality of sanitaryware increases, improvements of these functions are requisite and, therefore, many recent studies have focused on the surface properties of these products. Studies vary from changing the properties of the starting mixture (raw material type, particle size), firing conditions [1–5], addition of antibacterial compounds or salts [6–8], creating hydrophobic and oleophobic surfaces [9, 10]or a combination of these conditions [11].

Higher refractive index (1.92–1.97), wear-impact resistance, thermal shock and the chemical durability of zircon impart excellent properties to the surface of sanitaryware glaze [12, 13]. Owing to the high cost of zircon, several studies have been conducted aiming to reduce its usage or completely replace it by more economical alternatives. Despite these studies, zircon is still one of the main raw materials used in the sanitaryware industry. The effect of zircon on the functions of sanitaryware has therefore been well investigated. A certain amount of zircon should be used to enhance chemical and wear resistance. As the addition of zircon becomes greater than 10% mass, a higher resistance against alkali and acidic solutions is obtained [14]. ZrO_2 is a highly durable oxide against ion exchange and alkaline attack. Since the soluble of the ionic compound, such as ZrO^{+2}, Zr^{+4} and $HZrOO^{-3}$, form only lower and higher pH values, ZrO_2 based raw materials are preferred in order to obtain glazes with high chemical resistance [15]. The particle or grain size of zircon is another parameter studied and it directly affects optical properties and wear resistance. By decreasing the particle size of zircon, the possibility of a

© 2020 The Author(s). Published by IOP Publishing Ltd

Table 1. Oxide composition (wt%) of the industrial sanitaryware glaze.

Oxide (wt%)	LOI	SiO_2	Al_2O_3	TiO_2	Fe_2O_3	CaO	MgO	Na_2O	K_2O	ZnO	ZrO_2	BaO
Industrial Glaze	8.71	58.55	9.69	0.21	0.06	9.82	1.15	1.52	1.72	0.45	6.30	1.56

light-particle interaction increases and this will consequently increase light scattering [16]. In addition, the distribution of the zircon particles is important. A non-uniform distribution of zircon forms clusters that results in a glassy phase on the surface of glaze. A uniform distribution of zircon provides more sites for light scattering and increases L^* value [17]. The homogenous distribution of these hard crystals throughout the surface leads to an enhancement on the hardness of glaze [18].

Several approaches have been taken in order to obtain antibacterial surfaces; antibacterial agent release (e.g. silver coatings), contact killing (e.g. TiO_2 based materials) and anti-adhesion/bacteria-repellent. The use of molecules provides anti-adhesion or tailoring surface topography [19]. One way to tailor surface topography is to decrease the surface roughness that inhibits the attachment of bacteria cells by reducing the contact area between the cells and the surface area. When the dimension of surface topography is less than the cells (in the range of submicron or nano), the attachment of the cells is inhibited. In addition, submicron surface topography creates repulsive forces between bacteria and surface that reduce the possibility of attachment [20].

In the current study, the effect of the particle size of zircon on surface properties (whiteness, microstructure, roughness and bacterial activity) of sanitaryware glaze is investigated. As the particle size of zircon decreases to submicron scale, improvements in surface properties are obtained owing to a uniform distribution of zircon and reduced roughness values.

2. Experimental procedure

2.1. Sample preparation

Zircon (Zircobit MO, Bittosi, Italy) was milled four different times; for 0, 5, 15 and 25 min, to observe the effect of zircon particle size on surface properties, using ZrO_2 balls (3 mm in diameter) and ZrO_2 jar in a planetary ball mill (Retsch, PM4, Germany) at 450 rpm. Milled zircon powders were added to an industrial sanitaryware glaze and glaze suspensions were prepared using an eccentric jar mill, mixed with water (30 wt%) and binder (carboxy methyl cellulose) for 17 min. The oxide composition of industrial glaze is given in table 1, and glazes are designated as GZ-0, GZ-5, GZ-15, and GZ-25 regarding the zircon milling time.

Green sanitaryware bodies of 10 $\times$ 10 cm were coated by prepared glaze suspension being sprayed in 25 g amounts. The glazed samples were kept at room temperature for 2 h, then dried at 110 °C for 24 h. The samples were then sintered in an industrial tunnel kiln at 1220 °C for 16 h.

2.2. Characterization

The particle size distribution values of the zircon powders were measured using the laser diffraction technique (Malvern Mastersizer E 2000, UK). L^*, a^* and b^* parameters were measured with a colorimeter (Konica Minolta Chroma Meter CR-400, Japan).The distribution of zircon grains and the overall surface appearance were also examined by scanning electron microscopy (SEM) (Zeiss Supra 50 VP, Germany). SEM images were segmented by thresholding and analyzed automatically using Image J 1.52a software. Since the grains were not perfectly round, a minimum feret diameter of 250 grains from each sample was measured and then the average grain size was calculated. Chemical investigations of vitreous phase were performed using SEM with energy dispersion x-ray spectrometry (SEM–EDX) (Hitachi SU5000, Japan). X-ray diffraction (Rigaku MiniFlex, Japan) was performed using monochromatic Cu-Kα radiation ($\lambda = 1.5406$ Å).

The surface roughness of the glazed samples was characterized by atomic force microscopy (AFM) (QScope-250, Canada) using a non-contact mode equipped with a Si_3N_4 cantilevered scanner of 50 $\times$ 50 μm scan size. The surface roughness was evaluated by measured values of the root mean square roughness (Rq) and the average roughness (Ra). Rq is the standard deviation of the height values from the average height in the image. Ra is the mean height value as calculated from the entire surface plane.

The hardness of the glaze was measured by the indentation method (Shimadzu HMV-G, Japan). The measurement was carried out using a diamond indenter with a 10 N load for ten seconds.

2.3. Antibacterial-activity test

The antibacterial activity of the GZ-0 and GZ-25 samples against *Escherichia coli* and Staphylococcus Aureus was examined according to ISO 22196 (measurement of antibacterial activity on plastics and other non-porous surfaces) [21]. Prior to antibacterial activity test, both samples were sterilized. Bacterial suspensions were

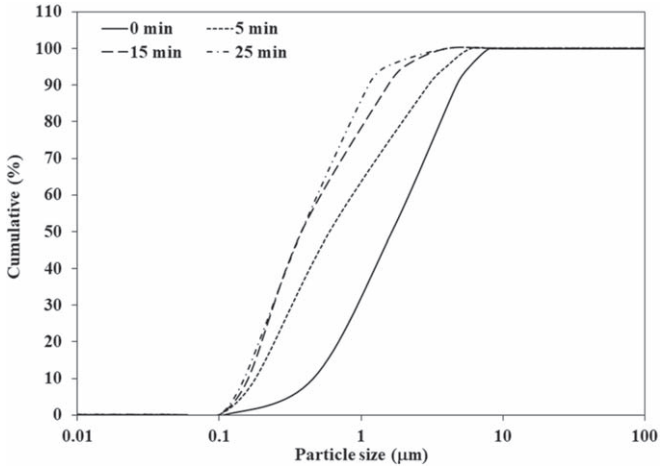


Figure 1. Cumulative particle size distribution of zircon powders against milling time.

Table 2. *a* b* parameters of glazed samples with different milling times.

Glazed Sample	L*	a*	b*
GZ-0	89.09	−0.22	2.01
GZ-5	90.03	−0.30	2.01
GZ-15	90.27	−0.24	1.64
GZ-25	91.47	−0.32	1.56

pipetted on the surface of samples then the surfaces were covered with sterilized plastic film. Incubation was done at a temperature of (35 ± 1) °C and a relative humidity of not less than 90% for (24 ± 1) h.

The test was conducted at the Saniter Laboratory (Istanbul, Turkey), which is accredited by the Turkish Accreditation Agency.

The number of viable bacteria was quantified by elapsed time (t = 0 h, t > 24 h) with the following equation being used for the calculation of antibacterial activity:

$$R = \log\left(\frac{B}{A}\right) - \log\left(\frac{C}{A}\right) = \log\left(\frac{B}{C}\right) \quad (1)$$

where R represents antibacterial activity, A is the average number of viable bacteria immediately after inoculation on the control specimen, B is the average number of viable bacteria on the control specimen after 24 h, and C is the average number of viable bacteria on the samples (GZ-0 and GZ-25) after 24 h.

3. Results and discussion

Planetary ball mills produce high energy density via rotation of the supporting disk and rotation of the jars in counter direction in the ratio 1:2. This difference in speeds forms an interaction between frictional and impact forces that causes high dynamic energies. Due to these forces high and very effective degree of size reduction of the planetary ball mill. Therefore, it is commonly used during the particle size reduction down to the nm scale [22–24]. Mia *et al* examined the grinding rate of a gibbsite powder by using a planetary ball mill. The median diameter of the powder was 51.1 μm and at the highest speed within 5 min the particle size reduced to one tenth of the initial size [25]. This demonstrates how efficiently planetary ball mill grinds ceramic powders in a short period of time.

The effect of milling time on the particle size distribution of zircon can be seen in figure 1. The median particle size of the non-ground zircon was measured as 1.65 μm (average particle size: 1.74 μm, with it decreasing to 0.45 μm (average particle size 0.48 μm) after 5 min. Since the practical grinding limit was approached after 15 min, the median particle size became constant at 0.38 μm (average particle size: 0.32 μm) for 15 and 25 min

According to L* a* b* parameters (table 2), the whiteness of the glazes showed a slight increase against a reduction in the particle size of the zircon. When zircon is added directly into a glaze formulation, fine zircon

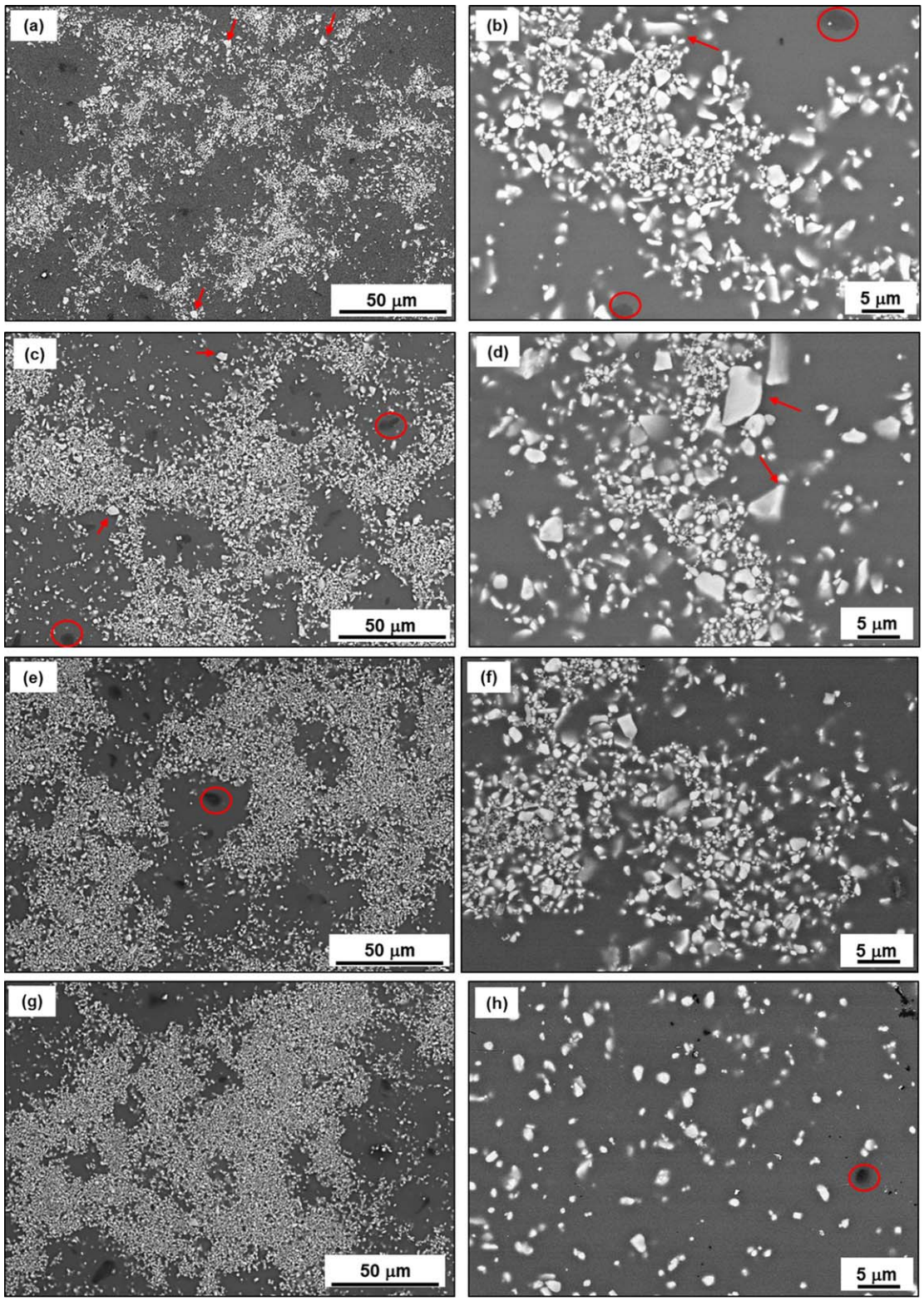


Figure 2. BSE images of glazed surfaces; (a) GZ-0 at 500×, (b) GZ-0 at 5000×, (c)GZ-5 at 500×, (d)GZ-5 at 5000×, (e) GZ-15 at 500×, (f) (c)GZ-15 at 5000×, (g) GZ-25 at 500× and (h) GZ-25 at 5000×.

particles are always favorable for high opacity and whiteness. The measured L^* values for these types of glaze vary between 89–93and the results given in table 2 are compatible with previous studies [14, 17]. If zircon particles are ofa particle size inthe range of 0.60–0.75 μm and an aspect ratio of around 1, the number of possible sites that diffract an incident light beam increases with higher opacity and whiteness being approached [3, 17]. Schabbach *et al* studied the relationship between zircon particle size and glaze color. They used three different particle sizes (200, 100 mesh and micronized) of zircon opacifier at a 5 wt% amount, and found that L^* values rose with

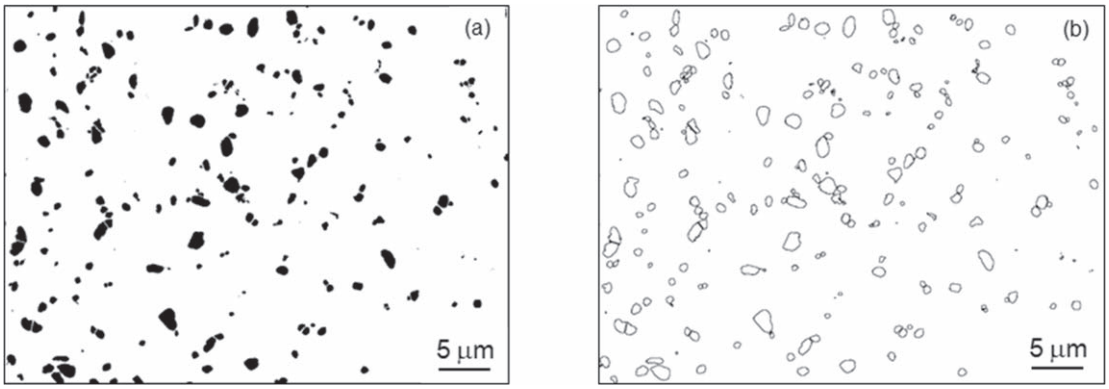


Figure 3. (a) Segmented and (b) analyzed images of BSE image of GZ-25.

decreasing particle size [16]. GZ-0 is the industrial production glaze at Kaleseramik A Ş Thanks to the increased whiteness value of zircon grain size reduction, the same whiteness value can be obtained using less zircon. Therefore, glaze cost can be reduced.

The significant effect of milling can be seen from the BSE images of samples that are presented in figures 2(a)–(h). Larger, bright zircon grains (indicated by arrow) were poorly distributed in GZ-0 from figures 2(a) and (b). When milling was applied for 5 min, micron-size zircon particles still existed in microstructure as given in figures 2(c) and (d). Cluster of zircon crystals was observed for these samples. Zircon clusters are the results of the combination effects of gas evolution and liquid phase formed during sintering. In the elimination step of bubbles, they make zircon grains to move and accumulate at the grains boundaries. As gas releasing is completed, zircon crystals are not able to return their initial position [17]. After milling for 15 and 25 min, these micron-size zircon grains were almost disappeared. Also, uniform distribution of zircon was obtained for both samples as shown in figures 2(e) and (g). The finer size of zircon can be beneficial to return its original location. This uniform distribution had important contribution to improve the surface properties of sanitarywares. Some dark regions (indicated by circles) were observed around the zircon particles for all samples. Two explanations were given for the formation of these zones. The presence of residual quartz may form such regions. Wang *et al* showed that formation of cracks was observed around the grain boundaries when residual quartz existed due to thermal expansion differences between the phases. The other explanation on the formation of these zones was generation of bubbles. These were the regions where bubbles have been eliminated from the surface. The remaining areas were refilled with the liquid phase that was formed at the sintering temperature [17].

The average grain size of zircon for all samples was measured from processed BSE images. Representative segmented and analyzed images of GZ-25 are shown in figures 3(a), (b). The measured grain size values from GZ-0 to GZ-25 are 1.49 μm, 1.53 μm, 0.57 μm and 0.33 μm, respectively. Castilone *et al* identified a critical zircon amount (>3wt%) for the recrystallization of zircon grains. Recrystallization occurs via dissolution of fine zircon particles and the subsequent coarsening of undissolved zircon particles [26]. Since the amount and size of the coarser zircon particles was lower for GZ-15 and GZ-25, the final zircon grainsize lowered for both samples.

As the size of zircon grains reduced, possible dissolution of these grains in the liquid phase might be observed. Blonski *et al* showed the relation between size and dissolution behavior of zircon opacifier and pigments. The dissolution rate was slightly higher than 2.5% when the size was over 10 μm. As size decreased to 1 μm, the increase in dissolution was 2% [kongre kitabı]. To observe dissolution behavior of zircon, the chemical composition of vitreous phase for all samples was analyzed by EDX and the results are represented between figures 4(a) and (h). Spectrum 1–4 correspond to the vitreous phases in glazed surfaces. Obtained EDX spectra and chemical analysis revealed that chemical compositions of vitreous phase were similar. The wt% of Zr varied from 1.6 to 2.1, no relation can be established between grain size and Zr content.

The x-ray diffraction (XRD) analyses of samples are presented in figure 5. According to XRD result, all samples contain zircon as a single phase. It must be pointed out that the intensity of the major peak of zircon from (200) increased against decreasing in zircon grain size. This proves the effect of milling on the distribution zircon grains. Since the finer zircon resulted uniform distribution on the surface, enhanced reflections from tetragonal zircon crystals from (200) was obtained.

Homogeneous distribution of the zircon grains improved the Vickers hardness of GZ-25 to 6.3 GPa from 5.2 of GZ-0 as given in table 3. Yu *et al* measured the hardness of sanitaryware glaze consisting of nano scale ZrO_2 and a micron scale zircon of 7.54 GPa as a result of homogeneous distribution of hard crystals ZrO_2 [18]. It can

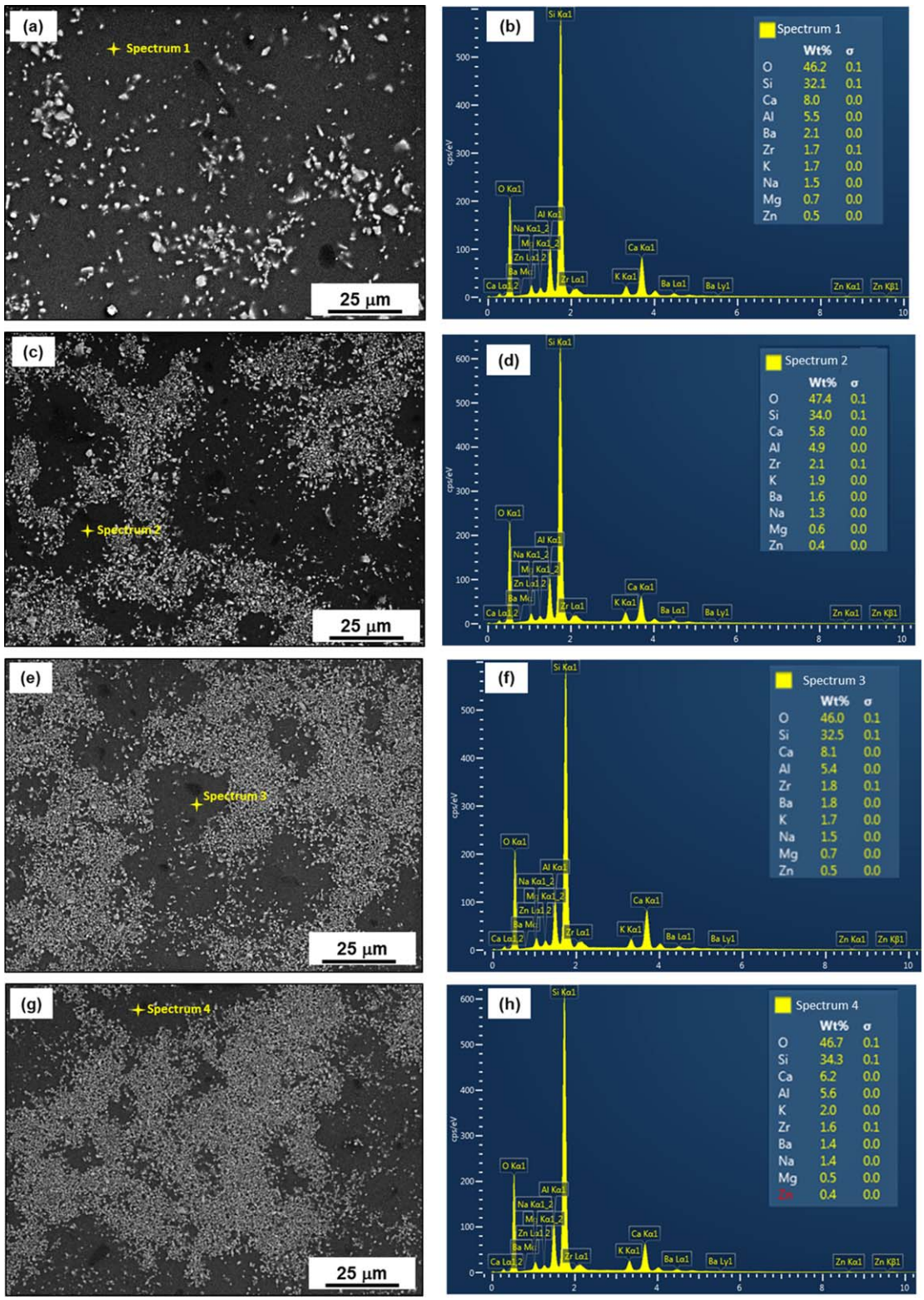


Figure 4. BSE images (showed the point of EDX analysis) and respective EDX spectrum of glazed surfaces; (a), (b) GZ-0 (c), (d) GZ-5 (e), (f) GZ-15, (g), (h) GZ-25.

be concluded that the contribution of the crystal phase on the hardness of glaze is more pronounced than for the glassy phase. Since the hardness of zircon is lower compared to ZrO_2, the values obtained in this study are acceptable [27].

Surface images of the glazed samples from the AFM analysis are shown in figures 6(a)–(d). The presence of large zircon grains can be seen in figures 6(a) and (b). In addition, it was detected that the accumulation of these grains increased the roughness of the glaze surfaces. As milling time rose to 15 and 25 min, even the elimination

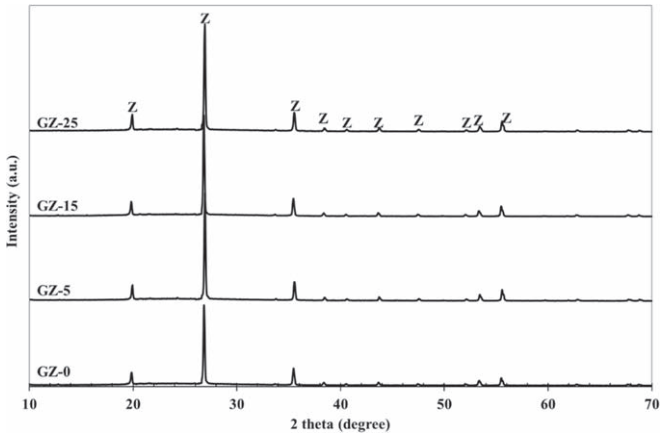


Figure 5. X-ray diffraction patterns of the glazed surfaces (Z: zircon).

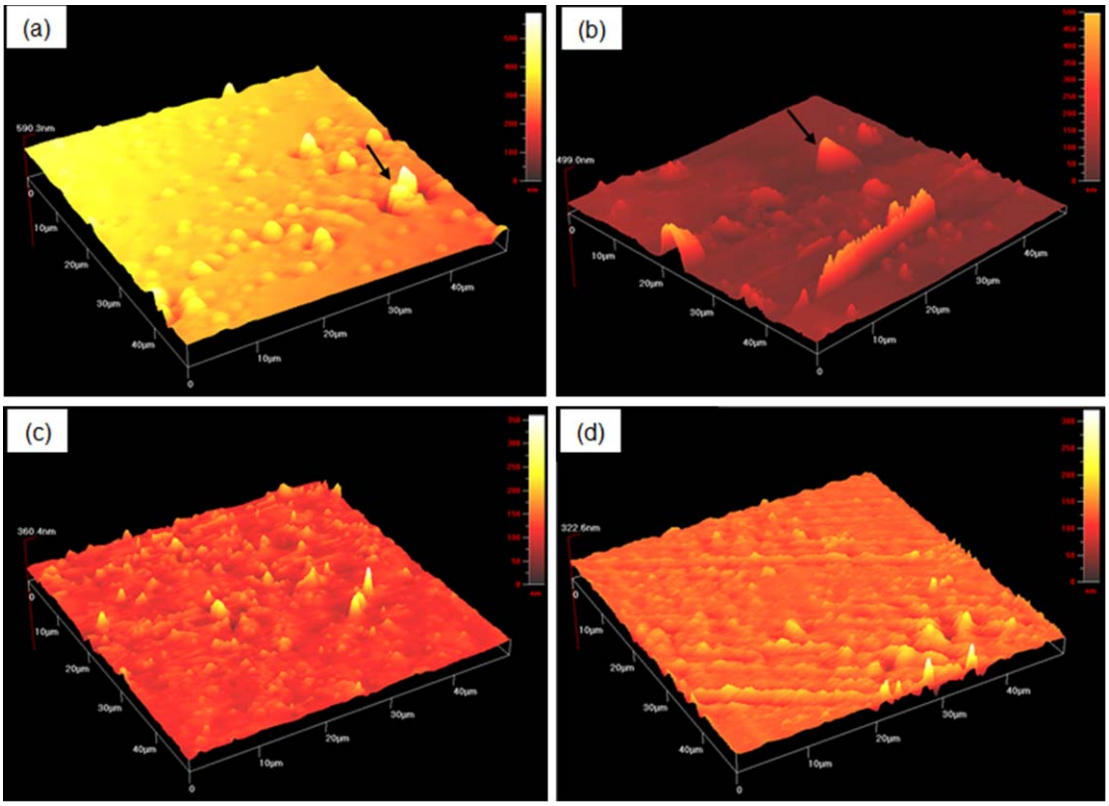


Figure 6. AFM images of glazed surface of different zircon grain size (a) GZ-0, (b) GZ-5, (c) GZ-15 and (d) GZ-25.

Table 3. Hardness values of glazed samples with different milling times .

Glazed Sample	Hardness (GPa)
GZ-0	5.2 (±0.4)
GZ-5	6.1 (±0.3)
GZ-15	6.3 (±0.4)
GZ-25	6.4 (±0.3)

of coarser zircon grains resulted in a reduction in roughness (figures 6(c) and (d)), although submicron scale roughness still appeared. As shown in table 4, the Rq and Ra values, milling provided a 28% smoother surface than non-milled.

Table 4. Rq-root mean square and Ra-average roughness of glazed samples.

Glazed Sample	Rq (nm)	Ra (nm)
GZ-0	49.70	39.51
GZ-5	42.31	24.40
GZ-15	16.09	11.02
GZ-25	16.23	10.94

Table 5. Antibacterial activity test results of sample GZ-0 and G-25.

Sample	Type of Bacteria	Inoculum density (cfu ml^{-1})	A (cfu cm^{-2})	B (cfu cm^{-2})	C (cfu cm^{-2})	R
GZ-0	Escherichia Coli (ATCC 8739)	1.32×10^5	9.2×10^4	7.1×10^4	2400	1.47
	Staphylococcus Aureus (ATCC 6538)	1.2×10^5	6.8×10^4	5.9×10^4	2700	1.35
GZ-25	Escherichia Coli (ATCC 8739)	1.9×10^5	1.2×10^4	4.3×10^3	90	1.65
	Staphylococcus Aureus (ATCC 6538)	3.1×10^5	9.7×10^4	6.1×10^3	70	1.94

The methods to impair the bacterial activity of a material can be done either active or passive ways. Active methods kill the bacteria while passive methods inhibit bacteria attachment. In this study, second method was examined by generating a smoother surface with less topographic features. It was anticipated that this type of surface can reduce the possible sites for bacterial attachment and subsequent biofilm formation. AFM measurement of GZ-25 showed that nanometric surface topography was generated and this inhibited the attachment by reducing the contact area between bacteria cells and the surface. Hence a great diminish was obtained in the number of viable bacteria for both types of the bacteria. Table 5 shows the antibacterial test results. The number of viable *E. coli* bacteria for GZ-0 was 2400, it dropped to 90 for GZ-25. A rapid decrease was also observed for S.Aures, smoother surface produced around a fortyfold decrease in the number of viable bacteria. Since all the R values are lower than 2, the samples did not show any antibacterial activity. However, a significant reduction was achieved due to the presence of submicron roughness as can be seen from the AFM image (figure 6(d)).

4. Conclusions

(1) The surface properties of opaque sanitaryware glaze are directly influenced by the initial particle size of zircon. Lower particle sizes resulted in a uniform distribution of zircon crystals on the surface and increased the whiteness (L^*) value.

(2) The hardness of the glaze was directly related to the distribution of zircon particles, and a lower initial size increased the hardness of the surface.

(3) The effect of milling was observed by AFM studies of the surfaces. The average roughness of GZ-0 was 39.51 nm, which decreased to 10.94 nm for GZ-25.

(4) A reduction in surface roughness provided an important contribution to the bacterial activity of the glazed samples. Even though the samples did not show any antibacterial activity, the amount of viable bacteria decreased by around twofold without the use of any antibacterial compound, such as silver or TiO_2.

Acknowledgments

Support from Kaleseramik Çanakkale Kalebodur Seramik San. A Ş is gratefully acknowledged.

The authors also acknowledge the support given by Abdullah Atılgan during the AFM study.

ORCID iDs

Gülsüm Topateş https://orcid.org/0000-0003-4453-8219

References

[1] Fröberg L, Kronberg T, Törnblom S and Hupa L 2007 Chemical durability of glazed surfaces *J. Eur. Ceram. Soc.* **27** 1811–6
[2] Bernasconi A, Diella V, Marinoni N, Pavese A and Francescon F 2012 Influence of composition on some industrially relevant properties of traditional sanitary-ware glaze *Ceram. Int.* **38** 5859–70
[3] Fröberg L, Kronberg T, Hupa L and Hupa M 2007 Influence of firing parameters on phase composition of raw glazes *J. Eur. Ceram. Soc.* **27** 1671–5
[4] Partyka J and Lis J 2011 The influence of the grain size distribution of raw materials on the selected surface properties of sanitary glazes *Ceram. Int.* **37** 1285–92
[5] Partyka J and Lis J 2012 Chemical corrosion of sanitary glazes of variable grain size composition in acid and basic aqueous solution media *Ceram. Int.* **38** 553–60
[6] Abe K, Tanaka M, Inaba S and Akimoto M 1996 Polyelectrolyte Complex Antibacterial Agent in Antibacterial Material *US Patent Number:* 5,578,598
[7] Surassmo S, Lauruengtana V, Kangwansupamongkol W and Ruktanonchai U 2007 Antibacterial effect of apatite coated titanium dioxide for textiles and coating amplications *Proc. of the 2nd IEEE Int. Conf. on Nano/Micro Engineered and Molecular Systems* pp 1012–5
[8] Uzgur E, Bayrakci F, Koparal S and Dogan A 2004 Applications of calcium phosphate based antibacterial ceramics on sanitary and tile wares *Key Eng. Mat.* **264–2 68** 1573–6
[9] Agné T 2007 Sanitary ware with easy cleaning and/or antibacterial properties *Tenside Surf. Det.* **44** 222–5
[10] Piispanen M, Kronberg T, Areva S, Joe P and Hupa L 2010 Easy-to-clean coatings on glass and glazed surfaces *Adv. Sci. Technol.* **66** 150–5
[11] Knies F, Schrantz K, Aneziris C, Gauckler L and Graule T 2016 Superhydrophilic ceramic glazes for sanitaryware *J. Ceram. Sci. Technol.* **7** 53–64
[12] Wang S, Peng C, Lü M and Wu J 2013 Effect of ZnO on crystallization of zircon from zirconium-based glaze *J. Am. Ceram. Soc.* **96** 2054–7
[13] Pina-Zapardiel R, Esteban-Cubillo A, Bartolomé J F, Pecharromán C and Moya J S 2013 High wear resistance white ceramic glaze containing needle like zircon single crystals by the addition of sepiolite n-ZrO_2 *J. Eur. Ceram. Soc.* **33** 3379–85
[14] Atkinson I, Smith M E and Zaharescu M 2012 Examining correlations between composition, structure and properties in zircon-containing raw glazes *Ceram. Int.* **38** 1827–33
[15] Eppler R A and Eppler D R 2000 *Glazes and Glass Coating* (Ohio: American Ceramic Society)
[16] Schabbach L M, Bondioli F, Ferrari A M, Manfredini T, Petter C O and Fredel M C 2008 Color in ceramic glazes: analysis of pigment and opacifier grain size distribution effect by spectrophotometer *J. Eur. Ceram. Soc.* **28** 1777–81
[17] Wang S, Peng C, Huang Z, Zhou J, Lü M and Wu J 2014 Clustering of zircon in raw glaze and its influence on optical properties of opaque glaze *J. Eur. Ceram. Soc.* **34** 541–7
[18] Yu Y, Su H, Peng C and Wu J 2019 Submicron-zirconia crystal-intergrown zircon opaque glaze *J. Eur. Ceram. Soc.* **39** 652–9 2019
[19] Cloutier M, Mantovani D and Rosei F 2015 Antibacterial coatings: challenges, perspectives, and opportunities, trends *Biotechnol.* **33** 637–52
[20] Feng G, Cheng Y, Wang S Y, Borca-Tasciuc D A, Worobo R W and Moraru C I 2015 Bacterial attachment and biofilm formation on surfaces are reduced by small-diameter nanoscale pores: how small is small enough? *Biofilms Microbiomes* **1** 1–9
[21] International Standard, Plastics—Measurement of antibacterial activity on plastics and non-porous surfaces, ISO 22196, 2007
[22] Burmeister C F and Kwade A 2013 Process engineering with planetary ball mills *Chem. Soc. Rev.* **42** 7660–7
[23] Broseghini M, Gelisio L, D'Incau M, Azanza Ricardo C L, Pugno N M and Scardi P 2016 Modeling of the planetary ball-milling process: The case study of ceramic powders *J. Eur. Ceram. Soc.* **36** 2205–12
[24] Real C and Gotor F J 2019 Effects of the speed ratio on the efficiency of planetary mills *Heliyon* **5** 3–14.
[25] Mio H, Kano J, Saito F and Kaneko K 2004 Optimum revolution and rotational directions and their speeds in planetary ball milling *Int. J. Miner. Process.* **74S** S85–92
[26] Castilone R J, Sriram D, Carty W M and Snyder R L 1999 Crystallization of Zircon in stoneware glazes *J.Am.Ceram.Soc.* **24** 2819–24
[27] Garrido L B, Aglietti E F, Martorello L, Camerucci M A and Cavalieri A L 2006 Hardness and fracture toughness of mullite-zirconia composites obtained by slip casting *Mater. Sci. Eng.* A **419** 290–6